Available online at www.sciencedirect.com
SCIENCE DIRECT®
Spectrochimica Acta Part A 59 (2003) 1805–1813
SPECTROCHIMICA ACTA PART A
www.elsevier.com/locate/saa

Experimental and computational studies of the structure and vibrational spectra of pyridinium-betaine of squaric acid

Tsonko M. Kolev *, Denitsa Y. Yancheva, Bistra A. Stamboliyska

Institute of Organic Chemistry, Bulgarian Academy of Sciences, Bulding 9, Bonchev str., 1113 Sofia, Bulgaria

Received 22 August 2002; received in revised form 12 November 2002; accepted 13 November 2002

Abstract

The FTIR spectra of pyridinium-betaine of squaric acid in 4000–100 cm^{-1} frequency region in solid state were measured. In addition, the structure and harmonic vibrational frequencies of this molecule were theoretically evaluated using restricted Hartree–Fock and B3LYP density functional methods. The computed vibrational frequencies are used to determine the types of molecular motions associated with each of the experimental bands observed. Comparison with the experimental spectra provides important information about the ability of these computational methods to describe the vibrational modes in these highly polar strained ring compounds.

Keywords: Vibrational spectra; Ab initio force field; Electronic structure; Band assignment

1. Introduction

Pyridinium-betaine of squaric acid (PBSQ) has been synthesized and described by Schmidt et al. in 1984 [1]. The authors have published only the melting points of the product, recrystallized from water (m.p. 279 °C) and from ethanol (225 °C) and obtained with very good yield [1].

PBSQ represents a new type of compound of squaric acid betaines. The classic betaine structure is associated with zwitterionic compounds consisting of an anionic carboxylate group and positively charged quaternary ammonium moiety. Zwitterions are electrically neutral molecules, however they differ substantially from other nonionic compounds in both structure and properties [2]. In terms of the structure, substituent groups with opposite charges can be easily distinguished. The two groups are separated by an electrically neutral skeleton and are not electronically conjugated with each other (via the mesomeric inductive or other effects).

In the case of PBSQ the two charges are part of one conjugated system and we can expect different spectral properties. The PBSQ are characterized with negative solvatochromism, e.g. in dichloroethane two strong bands at 372.5 and 390.0 nm as well as a weak band at 515 nm is observed; in ethanol λ_{max} are at 352.6 nm (strong) and 476 nm (weak); in acetonitrile 362.3 and 373.6 nm (strong)

* Corresponding author. Tel.: +359-2-9606-106; fax: +359-2-700-225.
E-mail address: kolev@orgchm.bas.bg (T.M. Kolev).

1386-1425/02/$ - see front matter
doi:10.1016/S1386-1425(02)00411-0

and 496 nm (weak); in water 339.4 nm (strong) and 443 nm (weak) [3]. The UV vis spectral data shows that this class of compounds has potential NLO activity. In this work, we report the results from FTIR spectra in solid state and the result from the ab initio and DFT calculations on the harmonic force field of PBSQ. The calculated vibrational frequencies are compared with those observed experimentally.

2. Experimental

The preparation of PBSQ is described in Ref. [1]. The product is purified by recrystallization from ethanol. The melting point of the compound studied coincides with the published literature [1]. The crystals are stable under normal conditions. The vibrational spectral data for the parent pyridine are taken from Ref. [4]. The IR spectra of the compound studied were recorded in the solid state in KBr and CsI pellets on a Bruker IFS-113v spectrometer equipped with high intensity Globar source Ge/KBr beam splitter and DTGS detector. The FIR spectra have been recorded on the same spectrometer equipped with high-pressure Hg are lamp a 6.25 er 25 μm Mylar beam splitter and DTGS detector. In both cases, the spectra have been recorded at a resolution of 1 cm^{-1} (100 scans).

3. Computations

Ab initio restricted Hartree–Fock (RHF) methods and density functional theory (DFT) are used to obtain equilibrium geometry, force field and fundamental vibrational frequency of PBSQ molecule. All calculations have been performed with the standard Gaussian [5] software (AIX, version 1998). The DFT method employed in the present study is B3LYP-Becke's three-parameter hybrid method [6] using the correlation functional of Lee et al. [7]. The standard 6-31G* basis set was applied in all calculations. It is well known that both RHF and B3LYP methods overestimate the frequencies of fundamental vibrations significantly. Thus, for a better correspondence between experimental and calculated values, the RHF and B3LYP results were modified using the empirical scaling factor, reported by Scott and Radom [8].

4. Results and discussion

4.1. Vibrational assignment

The fragment of the IR spectrum of PBSQ in 3200–2000 cm^{-1} in KBr pellets is shown in Fig. 1. The middle IR spectrum of the same compound in KBr disc is shown in Fig. 2. The FIR spectrum in 400–100 cm^{-1} in CsI matrix of PBSQ is shown in Fig. 3. The numeric values of experimental frequencies are compared with the corresponding RHF/6-31G* and B3LYP/6-31G* values in Table 1. The computed vibrational frequencies are used to determine the types of molecular motion associated with each of the observed experimental bands. The assignment of vibrational bands of the pyridinium moiety is denoted by Py, whereas that of squarate is designated by Sq. As can be seen from Table 1, the agreement of the calculated frequencies with the experimental data is very good. Mean absolute deviations between experimental and theoretical values are 14 and 25 cm^{-1} for the B3LYP and RHF calculations, respectively. DFT method provided more accurate vibrational spectra than the RHF methods. Hence, the abbreviated mode description provided with band assignments here are based on the B3LYP calculations.

The molecule of PBSQ has C_{2V} symmetry. As a result, PBSQ possesses 48 normal vibrations distributed in:

$$\Gamma = 17A_1 + 5A_2 + 10B_1 + 16B_2.$$

All bands are Raman and IR active except for A_2 symmetry class forbidden in the IR spectrum.

4.1.1. Vibrational assignment of pyridinium moiety

Assignments of bands in the experimental spectrum are carried out on the basis of previous work for pyridine [4] as well as calculations presented here.

Four stretching ν(CH) viz. 2, 13, 7 and 20b modes were observed in the IR spectrum of PBSQ.

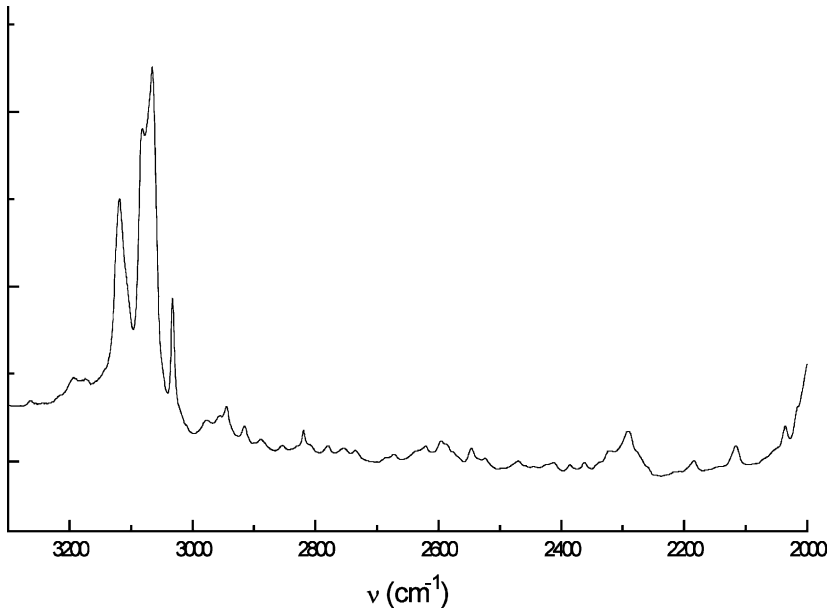

Fig. 1. Infrared spectrum of PBSQ (6 mg in 200 mg KBr) in 3200–2000 cm^{-1} frequency region.

The band corresponding to 20a vibration predicted by B3LYP/6-31G* as a very weak band is not observed in the experimental data. The frequencies of these vibrations indicate a general trend toward the increase of ν(CH) in PBSQ compared to the parent pyridine molecule. No

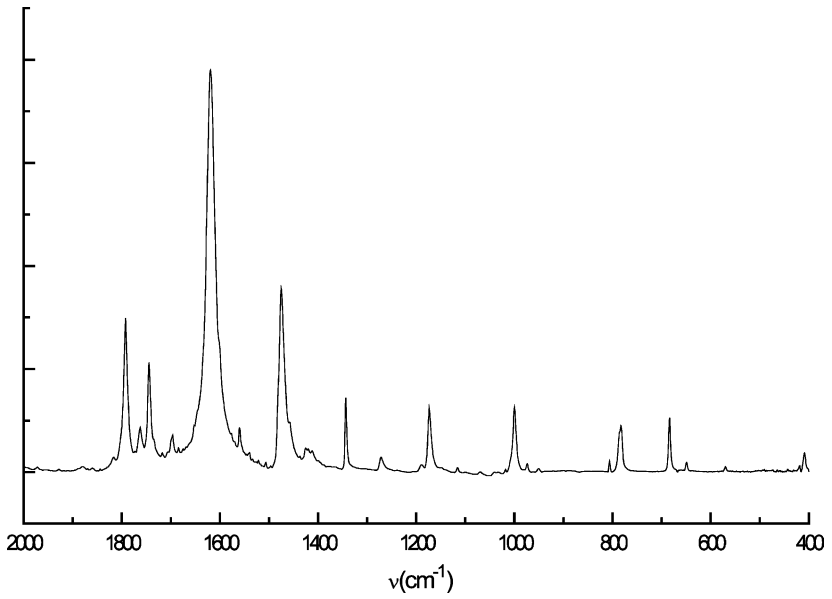

Fig. 2. Infrared spectrum of PBSQ (1 mg in 200 mg KBr) in 2000–400 cm^{-1} frequency region.

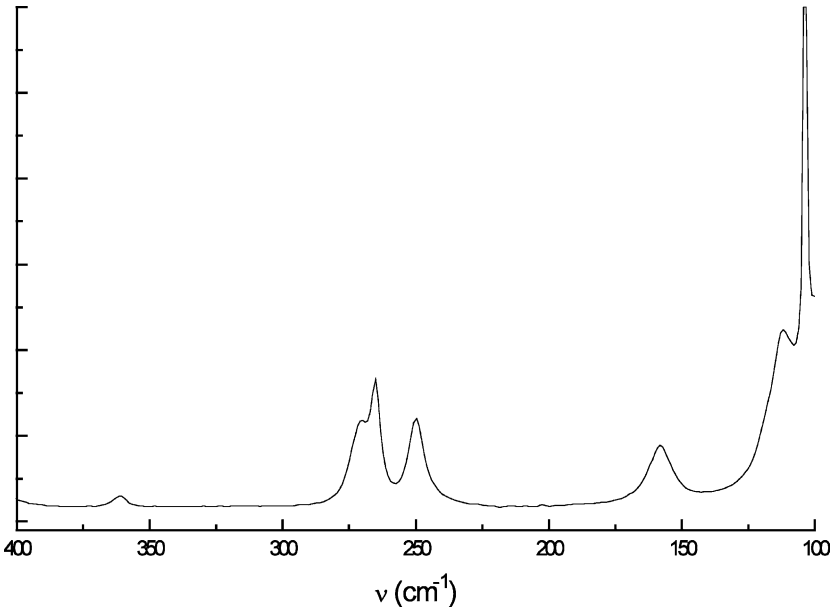

Fig. 3. Infrared spectrum of PBSQ (6 mg in 200 mg CsI) in 400–100 cm^{-1} frequency region.

significant change in the intensity of the band was observed with the transition from the neutral pyridine into PBSQ.

The normal vibrations of predominantly ring C–C stretching character viz. 8a, 8b, 19a and 19b have been predicted quite correctly by B3LYP method (mean absolute deviation is 8 cm^{-1}). The most intensive band in the IR spectrum of PBSQ at 1615 cm^{-1} was assigned to vibration 8a. The frequency of this mode is exactly predicted by B3LYP method (1617 cm^{-1}). This too high intensity is obviously due to vibronic coupling in the molecule studied. The very strong bands in IR spectra in this frequency region and resonantly enhanced bands in the IR and Raman spectra mainly correspond to the vibrations having a form of transition between aromatic- and quinone-like structure [14]. Among them especially the phenyl vibration 8a in the frequency region 1580–1620 cm^{-1} is often observed in the IR spectra of radical ions generated from aromatic ketones [15]. On the other hand, high NLO efficiency of radical ions has been reported by Meerholz et al. [16]. Hence, our assignment is in good agreement with the literature data [17]. At the RHF and B3LYP levels, well-known problems mainly concern the frequencies of 4 and 14 modes (Wilson's notation) [10]. Whereas the frequency of 4 mode seems to be reliable 668 cm^{-1} (RHF), 672 cm^{-1} (B3LYP) and observed frequency at 683 cm^{-1}, the failure with a correct description of the Kekule type mode has evidently basic reason [11–13]. Besides, even with large basis sets the overall correspondence with the experimental data remains poor.

The C–H in-plane deformation vibrations: 3, 9, 15, 18a, 18b in the experimental spectrum are found in the frequency region of 1342–1038 cm^{-1}, which is in agreement with the theoretical data (Table 1). The in-plane normal mode 18b predicted at 1036 cm^{-1} (RHF), 1034 cm^{-1} (B3LYP) is observed as a doublet at 1042/1048 cm^{-1}.

The frequencies of the normal mode 1 ('breathing') are predicted fairly well by theory: calculated 991 (B3LYP), measured 999 cm^{-1}. The predicted character of this normal mode has predominantly δ_{CCC} (Table 1).

The frequency region of C–H out-of-plane deformation vibrations 5, 17, 10a, 10b and 11 is predicted correctly: calculated 981–761 cm^{-1}, measured 976–790 cm^{-1}.

The deformation vibrations of the pyridinium ring: 4, 6a, 6b and 16a are in the frequency region

Table 1
Theoretical and experimental vibrational frequencies (ν in cm^{-1}) and IR intensities (A in km mol^{-1}) of PBSQ

No.	RHF	B3LYP		Expetimental	Character[b]	
	ν[a]	ν[a]	A	ν		
1.	3077	3116	4.6		ν(CH)	2
2.	3075	3110	0.2	3119	ν(CH)	20a
3.	3065	3102	4.8	3081	ν(CH)	13
4.	3061	3099	14.8	3066	ν(CH)	7
5.	3046	3095	0.8	3032	ν(CH)	20b
6.	1868	1804	404.3	1792	ν(C = O)	
7.	1796	1774	363	1762 1743	ν^{as}(C = O)	
8.	1676	1673	648.5	1697	ν^{as}(C = O)	
9.	1643	1617	35.7	1615	ν_{Py}(CC), δ_{Py}(CCH)	8a
10.	1581	1540	2.1	1559	ν_{Py}(CC), δ_{Py}(CCH)	8b
11.	1493	1476	115.4	1473	δ_{Py}(CCH), ν_{Py}(CC)	19a
12.	1477	1474	54.5	1466	δ_{Py}(CCH), ν_{Py}(CC)	19b
13.	1406	1391	200.6	1422 1417	ν(C-N), ν_{Sq}(CC)	
14.	1366	1349	6.2	1342	δ_{Py}(CCH)	3
15.	1215	1261	0.0	1270	ν_{Sq}(CC)	
16.	1203	1191	19.9	1189	δ_{Py}(CCH)	9a
17.	1171	1171	27.0	1172	δ_{Py}(CCH)	
18.	1118	1143	4.6	1149	δ_{Py}(CCC), δ_{Py}(CCH), δ_{Sq}(CCO)	15
19.	1087	1095	0.8	1114	ν_{Sq}(CC), δ_{Sq}(CCO)	
20.	1060	1059	0.2	1067	δ_{Py}(CCH), δ_{Py}(CCC)	18a
21.	1036	1034	0.7	1042 1038	δ_{Py}(CCH), δ_{Py}(CCC)	18b
22.	1030	991	15.5	999	δ_{Py}(CCC) ν_{Py}(CH)	1
23.	1026	981	0.9	976	γ_{Py}(CCH)	5
24.	1003	970	0.0	944	γ_{Py}(CCH)	17
25.	1000	934	6.7		γ_{Py}(CCH)	10a
26.	997	915	52.0	896	δ_{Sq}(CCO), δ_{Sq}(CCC)	
27.	887	859	0.0	859 845	γ_{Py}(CCH)	10b
28.	861	845	0.1	806	τ_{Py}(CCCH), δ_{Sq}(CCO)	
29.	791	772	1.5		τ_{Sq}(CCCO)	

Table 1 (*Continued*)

30.	787	761	45.2	790	γ_{Py}(CCH)	11
31.	710	757	1.1	782	γ_{Sq}(CCO)	
32.	668	672	27.5	683	γ_{Py}(CCH)	4
33.	667	658	3.8	648	δ_{Sq}(CCC), δ_{Py}(CCC)	
34.	631	630	0.1	638	δ_{Py}(CCC), δ_{Py}(CCH)	6a
35.	628	616	0.5	621	δ_{Sq}(CCC), ν_{Sq}(CO)	
36.	612	572	0.0	569	τ_{Sq}(CCCO)	6b
37.	527	535	0.0		τ_{Sq}(CCCO), τ(CCCN)	
38.	405	401	0.0	409	τ_{Py}(CCCH)	16a
39.	399	393	13.9	378	τ_{Py}(CCCH), τ_{Sq}(CCCO)	
40.	392	385	6.2	362	δ_{Sq}(CCC), δ(CCN)	
41.	340	339	0.0		δ_{Sq}(CCO), δ_{Py}(CCH)	
42.	266	252	15.3	272	δ_{Sq}(CCO), δ_{Py}(CCH)	
43.	259	245	1.7	265	δ_{Sq}(CCO), ν(C-N)	
44.	235	225	6.2	250	τ_{Sq}(CCCO), τ_{Py}(CCCH),	
45.	115	130	3.7	~110	τ_{Sq}(CCCO), τ(CCNC),	
46.	114	112	0.1		δ_{Sq}(CCO), δ(CCN),δ_{Py}(CCH)	
47.	68	75	0.0		τ_{Py}(CCCH)	
48.	57	65	0.1		τ_{Py}(CCCH), τ(CCNC)	

[a]Scaled by 0.8953 (for RHF/6-31G*) and 0.9614 (for B3LYP/6-31G*) [8].
[b]From B3LYP calculations. Vibrational modes: ν, stretching; δ and γ, in-plane and out-of- plane bendings, respectively; τ, torsion. Wilson's notation is used for the phenyl modes.

672–401 cm^{-1} predicted 683–409. A good agreement between the computed and experimental frequencies of these modes is found in accordance with literature data [12,13,26]. The second component of vibrational pair 16 is probably not observable here.

4.1.2. Vibrational assignment of squaric acid moiety

Stretching vibrations corresponding to the carbonyl groups are expected for the PBSQ structure given above. The strong band at 1792 cm^{-1} can be attributed to the stretching vibration of 'pure' carbonyl group—$\nu(C_{10}=O_{17})$. B3LYP/6-31G* method give good coincidence with the calculated one at 1804 cm^{-1}. The crystal structure of 4-benzoylpyridinium-1-squarate [9] shows clearly the C_9O_{16} bond length and C_8O_{18} one are the same due to the mesomeric equalization. The two equivalent structures and the mesomeric one are shown in Scheme 1. The 1762 and 1697 cm^{-1} bands belong to the symmetric and asymmetric stretching vibrations of these two mutually connected oscillators. The predicted frequencies are at 1774 and 1673 cm^{-1} (B3LYP).

The band at 1422 cm^{-1} are predicted at 1391 (B3LYP), 1406 cm^{-1} (RHF). The vibration description is predominantly C–N, but at higher frequency than the one observed in pyridinium betaine from Szafran and Koput [17]. Essentially a higher frequency of PBSQ is caused by partially quinoide character of $N-C_{sq}$ bond (see Scheme 2). In-plane deformation of Sq moiety: found at 806 cm^{-1}, is predicted fairly well—861 cm^{-1} (RHF), 845 cm^{-1} (B3LYP). Mixed deformation vibration with the predominantly Sq character are predicted well at 658 cm^{-1} (RHF) and 667 cm^{-1} (B3LYP)—measured at 648 cm^{-1}. The weak band at 638 cm^{-1} is also a mixed one and is well predicted by the theory—630 cm^{-1} (RHF), 631 cm^{-1} (B3LYP). The theory predicts the band at nearly 530 cm^{-1}, which is out-of-plane C–C–O and C–C–N deformations. In the experimental spectrum, there is no band with the predicted

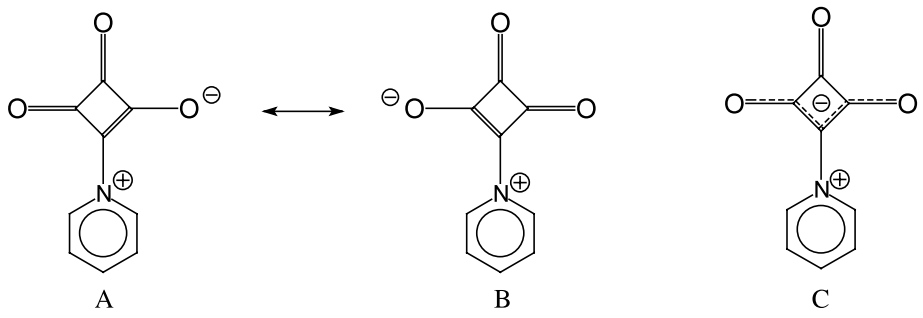

Scheme 1. Resonance contributors A and B and mesomeric structure C of PBSQ.

frequency. The band at 361 cm^{-1} belonging to in-plane deformation vibration with mainly C–C character is predicted quite well. The band at 340 cm^{-1} having purely C–C–C character of Sq moiety was not found in the spectrum. The strong bands at 271 and 265 cm^{-1} are assigned to deformation vibrations of Sq moiety and to mixed vibration, respectively. The strong band at 250 cm^{-1} and middle band at 158 cm^{-1} are assigned to out-of-plane vibrations of the same fragment.

4.2. Geometrical parameters

The bond length by mean of B3LYP method are given in Scheme 2. The bond lengths of Sq ring are influenced by valence strain. As can be seen from Table 2, the bond length of $C_{10}O_{17} = 1.195$ Å is in a good agreement with the 'pure' C = O bond, while the bond lengths C_9O_{16} and C_8O_{18} are equal because of mesomeric distribution of negative charge over this $O_{16}C_9C_7C_8O_{18}$ conjugated system. The interatomic distance $N–C_7 = 1.388$ is very close to the 'aromatic' CC one. The corresponding ν(CN) was assigned to the bands at 1417 cm^{-1}.

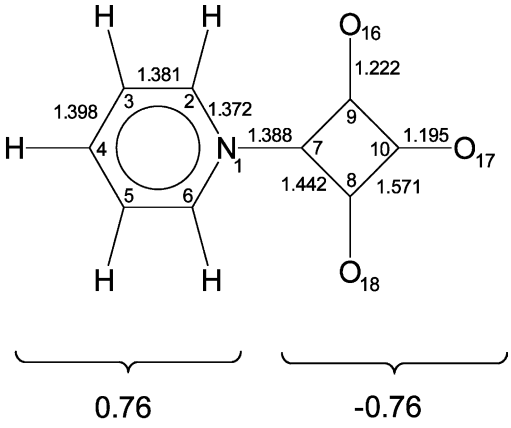

Scheme 2. Bond length (Å) and GAPT charges over Py- and Sq-fragments of PBSQ molecule calculated by B3LYP/6-31G*.

4.3. Electronic charges

The generalized atomic polar tensor (GAPT) model, first introduced by Cioslowski [18] was chosen for calculation of atomic charges. In this method, GAPT charge of atom α is an average trace of the atomic polar tensor:

Table 2
Calculated GAPT charges of PBSQ molecule by means of B3LYP/6-31G*

α[a]	Q^{α}
N^1	0.1811
C^2	0.1110
C^3	0.1736
C^4	0.1786
C^5	0.1736
C^6	0.1110
C^7	0.9279
C^8	1.0122
C^9	1.0122
C^{10}	1.0111
H^{11}	0.1457
H^{12}	0.0797
H^{13}	0.0757
H^{14}	0.0797
H^{15}	0.1457
O^{16}	−0.9742
O^{17}	−0.9200
O^{18}	−0.9742

[a] For atom numbering see Scheme 2.

$$Q^{\alpha} = \frac{1}{3}\left(\frac{\partial \mu_x}{\partial x_\alpha} + \frac{\partial \mu_y}{\partial y_\alpha} + \frac{\partial \mu_z}{\partial z_\alpha}\right)$$

The Q^{α} symbol will be applied to denote the GAPT charges. The calculated GAPT atomic charges are listed in Table 2. The potential nonlinearity of PBSQ, suggested by two charge transfer bands in UV vis spectrum of PBSQ, showing noticeable negative solvatochromism [3] as well as crystal structure of similar 4-benzoilpyridinium-1-squarate [9], is due to the charge transfer between positively charged pyridinium ring (0.76) and negatively charged Sq moiety (−0.76) (Scheme 2). It is known that *p*-nitroaniline (*p*-NA) is a typical push–pull molecule and it has significant second order hyperpolarizability [19,20]. The comparison of GAPT atomic charges in PBSQ molecule with those in reference molecule *p*-NA shows that the studied system expels *p*-NA [21]. We consider that the net charge distribution in the PBSQ molecule supports this statement.

It is well known in *p*-NA the charge flux (intramolecular charge transfer or CT) creates large permanent dipole moment (7.856 Debye) [21], whereas in PBSQ, the dipole moment amounts to 11.16 Debye (B3LYP/6-31G*) and 12.56 Debye (RHF/6-31G*). Thus, it can be expected that the molecule studied is a typical dipolar one and its first hyperpolarizability will be significantly greater than *p*-NA [20].

From the expression for the static vibrational hyperpolarizability within the double harmonic approximation it appears that the largest contributions to vibrational hyperpolarizability come from those normal modes that have the largest intensities both in IR and Raman spectra [22,23]. Del Zoppo et al. [24] and Champagne [25] have studied NLO properties of the *p*-NA molecule and they found a few bands of vibrations contributing to vibrational hyperpolarizability, which are simultaneously strong in IR and Raman spectra. These modes originate from the oscillation of the molecular structure between aromatic- and quinoid-like. We consider the middle bands at 271, 251 and 158 cm^{-1} and the strong band at 265 cm^{-1} corresponding to the vibrations already mentioned can be served for estimation of vibrational hyperpolarizability of PBSQ and for its comparison with electronic one.

5. Conclusions

The bands of IR spectrum of PBSQ were assigned with the help of force field calculations. The majority of the experimental frequencies are very well reproduced by the B3LYP/6-31G* method and satisfactorily by the HF/6-31G*. Comparison of the theoretical with the experimental spectra provides important information about the ability of these computational methods to describe the vibrational modes in these highly polar strained ring compounds.

The GAPT charges approach has been demonstrated by its application to PBSQ. On the basis of charge description analysis, it is concluded that in the isolated PBSQ molecule, the Sq moiety plays the role of electron donor and the pyridinium group of electron acceptor. It is found that the structure of PBSQ has an intermediate structure between the aromatic- and the quinoid-like one.

Acknowledgements

This work has been supported financially by DAAD-Bonn, Bad Godesberg, Germany; Bulgarian National Fund of Scientific Research, Contract X-801. Ts.K. thanks the Alexander von Humboldt Stiftung-Bad Godesberg (Germany) for financial support.

References

[1] A. Schmidt, U. Becker, A. Aimene, Tetrahedr. Lett. 25 (1984) 4475.
[2] R.G. Laughlin, Langmuir 7 (1991) 842 (and references cited therein).
[3] Ts. Kolev, D. Yancheva, St. Stoyanov, Chem. Mater. (submitted).
[4] K.B. Wiberg, V.A. Walters, K.N. Wong, S.D. Colsan, J. Phys. Chem. 88 (1994) 6067.
[5] M.J. Frisch, G.W. Trucks, H.B. Schlegel, G.E. Scuseria, M.A. Robb, J.R. Cheeseman, V.G. Zakrzewski, J.A. Montgomery, Jr, R.E. Stratmann, J.C. Burant, S. Dapprich, J.M. Millam, A.D. Daniels, K.N. Kudin, M.C.

Strain, O. Farkas, J. Tomasi, V. Barone, M. Cossi, R. Cammi, B. Mennucci, C. Pomelli, C. Adamo, S. Clifford, J. Ochterski, G.A. Petersson, P.Y. Ayala, Q. Cui, K. Morokuma, D.K. Malick, A.D. Rabuck, K. Raghavachari, J.B. Foresman, J. Cioslowski, J.V. Ortiz, A.G. Baboul, B.B. Stefanov, G. Liu, A. Liashenko, P. Piskorz, I. Komaromi, R. Gomperts, R.L. Martin, D.J. Fox, T. Keith, M.A. Al-Laham, C.Y. Peng, A. Nanayakkara, C. Gonzalez, M. Challacombe, P.M.W. Gill, B. Johnson, W. Chen, M.W. Wong, J.L. Andres, C. Gonzalez, M. Head-Gordon, E.S. Replogle, J.A. Pople, GAUSSIAN 98, Revision A.7, Gaussian, Inc, Pittsburgh, PA, 199573.

[6] A.D. Becke, Phys. Rev. A38 (1988) 3098.

[7] C. Lee, W. Yang, R.G. Parr, Phys. Rev. B37 (1988) 785.

[8] A.P. Scott, L. Radom, J. Phys. Chem. 100 (1996) 16502.

[9] Ts. Kolev, D. Yancheva, D.C. Kleb, M. Schürmann, H. Preut, P. Blechmann, Z. Kristallogr. NCS 216 (2001) 65.

[10] E.B. Wilson, Phys. Rev. 45 (1934) 427.

[11] H. Lampert, W. Mikenda, A. Karpfen, J. Phys. Chem. A101 (1997) 2254.

[12] Ts. Kolev, B.S. Stamboliyska, Spectrochim. Acta A56 (1999) 119.

[13] Ts. Kolev, B.S. Stamboliyska, Spectrochim. Acta A58 (2002) 97.

[14] M. Szostak, T. Misiaszek, R. Roszak, J. Rankin, R. Czernuszewicz, J. Chem. Phys. 99 (1995) 14992.

[15] I. Juchnovski, Ts. Kolev, Spectrosc. Lett. 18 (1985) 481 (and p. 471).

[16] K. Meerholz, J. Swiatkiewicz, P. Prasad, J. Chem. Phys. 99 (1995) 7715.

[17] M. Szafran, J. Koput, J. Mol. Struct. 381 (1996) 157.

[18] J. Cioslowski, J. Am. Chem. Soc. 111 (1989) 8333.

[19] J. Wolff, R. Wortmann, in: D. Bethell (Ed.), Organic Materials for Second-Order Non-linear Optics, Advances in Physical Organic Chemistry, vol. 32, 1999.

[20] H.S. Nalwa, S. Miyata (Eds.), Nonlinear Optics of Organic Molecules and Polymers, Chapter 4, CRC Press, Boca Raton, 1997.

[21] T. Misiaszek, M.M. Szostak, J. Mol. Struct. 526 (2000) 303.

[22] D. Bishop, Adv. Chem. Phys. 104 (1998) 1.

[23] C. Castiglioni, M. Gussoni, M. Del Zoppo, G. Zerbi, Sol. State Commun. 82 (1992) 13.

[24] M. Del Zoppo, C. Castiglioni, G. Zerbi, Nonlinear Opt. 9 (1995) 73.

[25] B. Champagne, Chem. Phys. Lett. 261 (1996) 57.

[26] G. Varsanyi, Assignment for Vibrational Spectra of Benzene Derivatives, Academic Press, New York, 1969.